THE UNDERWATER TOWED SYSTEM BEHAVIOR DURING SHIP TURNING MANEUVERS

Zhi-Jiang Yuan
Dept. of Navigation, Dalian Naval Academy, Dalian, China., yuanyr0531@163.com

Liang-An Jin
Dept. of Navigation, Dalian Naval Academy, Dalian, China.

Wei Chi
Dept. of Navigation, Dalian Naval Academy, Dalian, China.

Xiao-Gang Jiang
Dept. of Navigation, Dalian Naval Academy, Dalian, China.

Zhi-Lin Zheng
Dept. of Navigation, Dalian Naval Academy, Dalian, China.

Follow this and additional works at: https://jmstt.ntou.edu.tw/journal

Part of the Engineering Commons

Recommended Citation

THE UNDERWATER TOWED SYSTEM BEHAVIOR DURING SHIP TURNING MANEUVERS

Acknowledgements

THE UNDERWATER TOWED SYSTEM BEHAVIOR DURING SHIP TURNING MANEUVERS

Zhi-Jiang Yuan, Liang-An Jin, Wei Chi, Xiao-Gang Jiang, and Zheng Zhi-Lin

ABSTRACT

The depth and attitude of underwater towed system show complex behavior during the towing ship turning maneuvers. However, it remains unclear how the two indexes change when the coupling relationship between the cable and the towed vehicle is considered. Here, to solve this issue, and we develop a new numerical method that can be used to predict the behavior of towed system during towing ship turning maneuvers. Specially, a finite difference method and six-degree-of-freedom equations are used to describe the motion of towed cable and towed vehicle respectively. Based on the center finite difference method, the partial differential equations and differential equations are transformed to nonlinear algebra equations then the Newton iteration method is used to solve the nonlinear equations. Then, we simulate the transient behaviors of towed system during the towing ship making 180° and 360° with different turning radius, and find that the depth and attitude of towed system are affected by the towing ship turning maneuvers. We show that the smaller of the turning radius, the variations of depth and attitude are larger. Moreover, the new steady state can be achieved easily during the 360° turning maneuver. The numerical method and result that we derived can be applied to design the towing ship turning maneuvers, towed system and control method.

I. INTRODUCTION

Underwater towed systems have been widely utilized in the exploration of the underwater environment. In many types of applications, the systems include the towing ship, tow cable and towed vehicle. Normally, the towed vehicles are equipped with many types of ocean detecting instruments. The operation of instruments in towed system requires that the towed vehicle should be stable during a towing operation (Grosenbaugh, 2007;

Yuan et al., 2014, 2016). Whereas the nonlinear motion of a towing ship during the turning maneuvers is transmitted down the cable to the towed vehicle as well as the hydrodynamic forces on the tow cable and towed vehicle are nonlinear, which result in variations both of attitude and depth of the system relative to its steady state. Some researches showed that these vibrations can be sufficiently large to throw the towed vehicle off out of sea (Fossen, 1994). The towed vehicle of active towed linear array sonar loads acoustic array, which emits sound waves to detect the underwater object. When the attitude of the towed vehicle changes rapidly, the reflection of the sound waves can hardly be received and the detection capability of sonar is reduced. (Han et al., 2013). The towed vehicle of the side scan sonar emits conical or fan-shape pulses down toward the seafloor to produce the side-scan sonar imagery. The precision of sonar imagery depends on the depth between the towed vehicle and seafloor (Montefalcone et al., 2013). Therefore, the investigation about the variations both of depth and attitude of towed vehicle is crucial for a stable towing operation. It is a basis for maintaining the depth and attitude of a towed vehicle to satisfy the requirements of system under different turning maneuvers, which is one of the major concerns of users (Narasimhan and Singh, 2006). Due to their essential, intricate and interesting dynamic behavior, there has been growing interest in the research on the transient behavior of underwater towed system during the towing ship turning maneuvers.

Much of our current knowledge about the configuration of towed system during ship turning maneuvers can be attributed to the analyses of Choo and Casarella (1972), Chapman (1984) and Grosenbaugh (2007). The latter two papers gave some more profound and comprehensive views. Chapman calculated the steady state profile of a tow cable during straight tows and turned with different parameters. His work showed that a towed system underwent large transient motions as it entered and exited the turns, and defined a critical ship turning radius for a given towing speed. Below the critical turning radius, the underwater towed system effectively collapsed, which resulted in a large increase in the towed vehicle depth and a large decrease in the towed vehicle turning radius. Grosenbaugh also analyzed the stability of the towing configuration from a dynamic standpoint and developed an alternate definition for the transition point between large radius and small radius turning behavior. However, the towed vehicle used in the research of Chapman
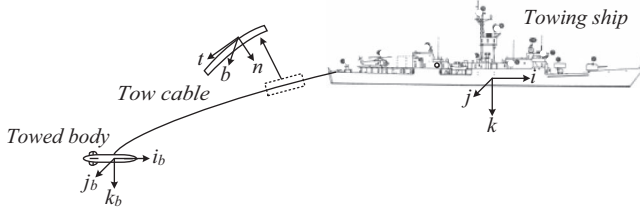
Fig. 1. Three coordinate frames of underwater towed system.

(1984), Grosenbaugh (2007) and Wang (2015) were treated as "heavy fish", i.e., the drag coefficient was set equal to zero. Their models of towed vehicle was simple and not fully three-dimensional (VanZwieten et al., 2006). In fact, the motion of a towed vehicle is strongly nonlinear and should be treated as a rigid body with six-freedoms (Fossen, 1994). For this reason, under the assumption in Chapman (1984) and Grosenbaugh (2007), it was hard to predict the transient behaviors of towed system precisely, and analyze the variation of the towed vehicle's attitude. Moreover, the stability of the towed vehicle can not be considered in the governing equation and simulation. Grosenbaugh pointed out that the towed vehicle depth oscillated with amplitude as the towing ship turning maneuvers. However, the variation of towed vehicle's depth must be coupled with attitude variation of towed vehicle (Fossen, 1994). When the pitch and roll deflection are great enough, the longitudinal and lateral stabilities can be caused losing. On the other hand, the variation of towed vehicle's attitude can influence on the data accuracy of towed system Fossen (2002). In marine geophysics, within common applications including the use of side-scan-sonar systems, and marine vector magnetometers and gravimeters, the pitch, roll angle may be required to meet the requirements (Fernandez et al., 2002).

The purpose of this paper will extend the idea of Chapman (1984) and Grosenbaugh (2007) by performing a detailed analysis of the transient behavior during the towing ship turning maneuvers. In this paper, in order to describe the hydrodynamic behavior of the towed vehicle in three-dimensions, we adopt the six-degree-of-freedom equations of motion for submarine simulation. These equations governing towed cable are adopted the classical finite difference method (Ablow and Schechter, 1983) that has become popular for solving ocean towing and mooring problems, which are then solved using a central finite difference method. In our paper, the Newton iteration method is used to solve this special form of finite difference equations. The transient behavior of cable towed system can be given out including the depth and attitude of towed vehicle. In addition, the stability of towed vehicle of towed vehicle can be considered in the simulation.

II. MATHEMATICAL FORMULATION

1. Coordinate Systems

To analyze the transient behavior of the underwater towed system, it is convenient to define three coordinate systems, i.e.,

the earth-fixed frame (i, j, k) and towed cable frames along the cable (t, n, b) and towed vehicle-fixed frame (i_b, j_b, k_b). As shown in Fig. 1, the earth-fixed frame (i, j, k) is selected with k pointing vertically downwards. The origin of the frames (i, j, k) and (t, n, b) is coincident. The orientation of the local frame is so chosen that t is tangent to the cable in the direction of increasing tow cable length coordinate s, b is in the plane of i and j, t and n lie in a vertical plane. The towed vehicle-fixed frame (i_b, j_b, k_b) is located at the buoyancy centre of the towed vehicle, with i_b coinciding with the longitudinal axis, and j_b pointing to starboard.

The relationship between the towed vehicle-fixed frame and the earth-fixed frame is expressed in terms of Euler angles (Feng and Allen, 2004), i.e.,

$$(i_b, j_b, k_b) = [i \ j \ k] R(\phi, \theta, \psi) \tag{1}$$

with

$$R(\phi, \theta, \psi) = \begin{bmatrix} c\theta c\psi & -c\phi s\psi + s\phi s\theta c\psi & s\phi s\psi + c\phi s\theta c\psi \\ c\theta s\psi & c\phi c\psi + s\phi s\theta s\psi & -s\phi c\psi + c\phi s\theta s\psi \\ -s\theta & s\phi c\theta & c\phi c\theta \end{bmatrix}$$

where $c = \cos$, $s = \sin$ and ϕ, θ, ψ are the roll, pitch and heading angle of the towed vehicle, respectively.

The relationship between the towed cable frames and the earth-fixed frame can be expressed as follows

$$(t \ n \ b) = [i \ j \ k] W(\alpha, \beta) \tag{2}$$

with

$$W(\alpha, \beta) = \begin{bmatrix} c\alpha c\beta & -c\alpha s\beta & s\alpha \\ -s\alpha c\beta & s\alpha s\beta & c\alpha \\ -s\beta & -c\beta & 0 \end{bmatrix}$$

The Eq. (2) is obtained by three rotations of the earth-fixed frame. Angle α represents the rotation angle about the k axis into the plane of t and n. Angle β represents the rotation angle about the b axis bring i and j into coincidence with t and n.

In terms of Eqs. (1) and (2), the relationship between the tow cable frames and towed vehicle-fixed frame is written as (Ablow and Schechter, 1983)

$$[t \ n \ b] = [i_b \ j_b \ k_b] R^T(\phi, \theta, \psi) W(\alpha, \beta) \tag{3}$$

2. Dynamic Equations

1) Cable Dynamic Model

The tow cable is a long elastic cylinder that only sustains tensile loads and its length varies with the time. Defining s as the vertical coordinate the balance of the forces (per unit length)

at any point of the tow cable is (Fernandez et al., 2002)

$$\frac{\partial}{\partial s}\boldsymbol{T} + \boldsymbol{W} + \boldsymbol{F} = m\boldsymbol{a} \tag{4}$$

where $\boldsymbol{T}(s)$ is the tension of the tether, $\boldsymbol{F}(s)$ is the hydrodynamic force, m is the mass per unit length and includes the added mass, $\boldsymbol{a}$ is the inertial acceleration.

The Eq. (4) can be represented by defining the vector

$$y(s,t) := \begin{bmatrix} T & V_t & V_n & V_b & \alpha & \beta \end{bmatrix}^T \tag{5}$$

where t and s denote the time and the arc length of the cable measured from the tow-point, respectively, T is the tension and $\boldsymbol{V}_c = \begin{bmatrix} V_t & V_n & V_b \end{bmatrix}^T$ denotes the velocity vector in the local frames along the cable. The cable dynamics can be expressed by the following partial differential equation:

$$M\frac{\partial y}{\partial s} = N\frac{\partial y}{\partial t} + q \tag{6}$$

2) Towed Vehicle Dynamic Model

The dynamic equations of towed vehicle are strongly non-linear, time varying, and uncertain in the parameters and include the Coriolis and centripetal kinematics coupling terms and the drag ones. The dynamic equations of motion of underwater towed vehicle have been presented by several authors (Fossen, 2002; Christina et al., 2014). Applying Newton's Second Law to the towed vehicle results in equations of motion of the form:

$$m\left[\dot{u} - vr + wq - x_G\left(q^2 + r^2\right) + y_G\left(pq - \dot{r}\right) + z_G\left(pr + \dot{q}\right)\right]$$
$$= X_H + X_W + X_C + X_T \tag{7}$$

$$m\left[\dot{v} + ur - wp + x_G\left(pq + \dot{r}\right) - y_G\left(p^2 + r^2\right) + z_G\left(qr - \dot{p}\right)\right]$$
$$= Y_H + Y_W + Y_C + Y_T \tag{8}$$

$$m\left[\dot{w} - uq + vp + x_G\left(pr - \dot{q}\right) + y_G\left(qr + \dot{p}\right) - z_G\left(p^2 + q^2\right)\right]$$
$$= Z_H + Z_W + Z_C + Z_T \tag{9}$$

$$I_x\dot{q} + \left(I_z - I_y\right)qr + I_{xy}\left(pr - \dot{q}\right) - I_{yz}\left(q^2 - r^2\right) - I_{xz}\left(pq + \dot{r}\right)$$
$$+ m\left[y_G\left(\dot{w} - uq + vp\right) - z_G\left(\dot{v} + ur - wp\right)\right]$$
$$= K_H + K_W + K_C + K_T \tag{10}$$

$$I_y\dot{q} + \left(I_x - I_z\right)pr - I_{xy}\left(qr + \dot{p}\right) + I_{yz}\left(pq - \dot{r}\right) + I_{xz}\left(p^2 - r^2\right)$$
$$- m\left[x_G\left(\dot{w} - uq + vp\right) - z_G\left(\dot{u} - vr + wq\right)\right] \tag{11}$$
$$= M_H + M_W + M_C + M_T$$

$$I_z\dot{r} + \left(I_y - I_x\right)pq - I_{xy}\left(p^2 - q^2\right) - I_{yz}\left(pr + \dot{q}\right) + I_{xz}\left(qr - \dot{p}\right)$$
$$+ m\left[x_G\left(\dot{v} + ur - wp\right) - y_G\left(\dot{u} - vr + wq\right)\right] \tag{12}$$
$$= N_H + N_W + N_C + N_T$$

where the left-hand sides represent inertial forces and moments and the right-hand sides denote external forces on towed vehicle. The symbols in the equations are based on the standard notation. The vector (u, v, w, p, q, r) is the generalized velocity vector in the towed vehicle-fixed frame. u, v and w are the translational velocities expressed in the body-fixed frame. p, q, and r are the rotational velocities expressed in the towed vehicle-fixed frame. It is assumed that the external forces $\boldsymbol{F}_0 = (X, Y, Z)^T$ and moments $\boldsymbol{M}_0 = (K, M, N)^T$ on a towed vehicle.

Subscript H reflects hydrodynamic contributions, W buoyant and weight effects, C forces arising from control surfaces (control wing, flap etc.) and T towing forces. The symbols in the equations are based on the standard notation.

The hydrodynamic forces acting on the towed vehicle are given by

$$X_H = X_{\dot{u}}\dot{u} - X_{uu}u|u| \tag{13}$$

$$Y_H = Y_{\dot{v}}\dot{v} - \frac{1}{2}\rho C_{Dv}D_v\int\left[\left(v + xr\right)^2 + \left(w - xq\right)^2\right]\frac{(v + xr)}{U_{cf}(x)}dx \tag{14}$$

$$Z_H = Z_{\dot{w}}\dot{w} - \frac{1}{2}\rho C_{Dv}D_v\int\left[\left(v + xr\right)^2 + \left(w - xq\right)^2\right]\frac{(w - xq)}{U_{cf}(x)}dx \tag{15}$$

$$K_H = K_{\dot{p}}\dot{p} \tag{16}$$

$$M_H = M_{\dot{q}}\dot{q} + \frac{1}{2}\rho C_{Dv}D_v\int\left[\left(v + xr\right)^2 + \left(w - xq\right)^2\right]\frac{(w - xq)x}{U_{cf}(x)}dx \tag{17}$$

$$N_H = N_{\dot{r}}\dot{r} - \frac{1}{2}\rho C_{Dv}D_v\int\left[\left(v + xr\right)^2 + \left(w - xq\right)^2\right]\frac{(v + xr)x}{U_{cf}(x)}dx \tag{18}$$

where C_D is the drag coefficient of the towed vehicle in sway and heave, D_v the diameter of the towed vehicle, and

$$U_{cf} = \left[\left(v + xr \right)^2 + \left(w - xq \right)^2 \right]^{1/2} \tag{19}$$

The integrals in the above equations are over the length of the towed vehicle.

Hydrostatic restoring forces and moments due to vehicle weight W and buoyancy B are given by

$$X_W = -\left(W - B \right) \sin \theta \tag{20}$$

$$Y_W = \left(W - B \right) \cos \theta \sin \phi \tag{21}$$

$$Z_W = \left(W - B \right) \cos \theta \cos \phi \tag{22}$$

$$K_W = \left(y_G W - y_B B \right) \cos \theta \cos \phi - \left(z_G W - z_B B \right) \cos \theta \sin \phi \tag{23}$$

$$M_W = -\left(x_G W - x_B B \right) \cos \theta \cos \phi - \left(z_G W - z_B B \right) \sin \theta \tag{24}$$

$$N_W = \left(x_G W - x_B B \right) \cos \theta \sin \phi + \left(y_G W - y_B B \right) \sin \theta \tag{25}$$

The towing forces and moments on the towed vehicle in local coordinates of the vehicle are

$$F_T = \begin{bmatrix} X_T \\ Y_T \\ Z_T \end{bmatrix} = -R^T \left(\phi, \theta, \psi \right) W \left(\alpha, \beta \right) T_{cable} \tag{26}$$

$$\left[K_T, M_T, N_T \right] = r_T \times F_T \tag{27}$$

where T_{cable} is towed force at the towed vehicle-end.

The six boundary conditions are required to specify the solution of governing equations. The immersed parted of the cable have two ends: the towed vehicle-end and the towing ship-end. The towed vehicle-end is located at the tail of the towed vehicle, while the towing ship-end is located at the tail of towing ship. Since the cable shares the velocity of the towed vehicle at towed vehicle-end and shares the velocity of towing ship at towing ship-end.

The velocity of the towed vehicle-end in the towed vehicle-fixed frame is $(V + \Omega \times r_c)$, where $\times$ denotes the cross product of two vectors. In terms of Eq. (3), the velocity of the towed vehicle-end can be repressed in the towed vehicle-fixed frame of the cable at the towed vehicle end, i.e.,

$$V_c \left(0, t \right) = W^T \left(\alpha, \beta \right) R \left(\phi, \theta, \psi \right) \left(V + \Omega \times r_c \right) \tag{28}$$

where involve three boundary conditions. The other three boundary conditions of tow ship-end can be expressed using the same style as the Eq. (28).

To complete the hydrodynamic model of the towed system,

the expression for the rates of change of Euler angles for the towed vehicle is (Christina et al., 2009)

$$\dot{\phi} = p + q \sin \phi \tan \theta + r \cos \phi \tan \theta \tag{29}$$

$$\dot{\theta} = q \cos \phi - r \sin \phi \tag{30}$$

$$\dot{\psi} = q \frac{\sin \phi}{\cos \theta} + r \frac{\cos \phi}{\cos \theta} \tag{31}$$

3. Numerical Scheme

The governing equations of towed system are composed of the Eqs. (6)-(12). These equations cannot be solved theoretically and so a numerical method is required. An implicit finite difference algorithm is employed for solving the three dimensional cable equations, and the Newton-Raphson iteration scheme is adopted for solving the non-linear problem. The numerical solutions of the partial differential Eq. (6) will be obtained by the finite difference method which discretizes the equations over time and space. The cable is first divided into n nodes separated by a distance Δs and time is divided into a series of duration Δt. Using the centered finite differences and evaluating Eq. (6) at mid-nodes $j + 1/2$ and at the time $i + 1/2$ give

$$\left[M_{j+1}^{i+1} + M_j^{i+1} \right] \frac{y_{j+1}^{i+1} - y_j^{i+1}}{\Delta s} + \left[M_{j+1}^i + M_j^i \right] \frac{y_{j+1}^i - y_j^i}{\Delta s}$$

$$= \left[N_{j+1}^{i+1} + N_{j+1}^i \right] \frac{y_{j+1}^{i+1} - y_{j+1}^i}{\Delta s} + \left[N_j^{i+1} + N_j^i \right] \frac{y_j^{i+1} - y_j^i}{\Delta s} \tag{32}$$

$$+ Q_{j+1}^{i+1} + Q_j^{i+1} + Q_{j+1}^i + Q_j^i$$

The finite difference equations include $(n + 1)$ cable nodes and $6(n + 1)$ cable nodes variables. There are $6n$ equations and the other 6 equations are necessary and obtained from the tow ship-end and towed vehicle-end boundary conditions. However, Eq. (28) introduces 9 new variables, that is 3 translational velocity components (u, v, w), 3 angular velocity components (p, q, r) and 3 Euler angles (θ, ϕ, ψ) of the towed vehicle. Therefore, 9 more equations are needed to solve the problem. These 9 equations are given by Eqs. (7)-(12) and Eqs. (29)-(31). The above equations are non-linear, and so it is necessary to solve the equations at each time step iteratively. In this work, the Newton-Raphson iteration scheme is applied (Fig. 2).

The nonlinear algebraic equation $\Phi(Y) = 0$ as established above has $6 \times (n + 1) + 9$ scalar equations. The unknown variables Y are orders as

$$Y = \left\{ y_{1:n+1}, \left(u, v, w, p, q, r, \phi, \theta, \psi \right) \right\}^T \tag{33}$$

The nonlinear algebraic equation $\Phi(Y) = 0$ is solved by iteration in the time domain as shown in the Fig. 2. The first step is formulating the dynamic model of towing cable Eq. (6)
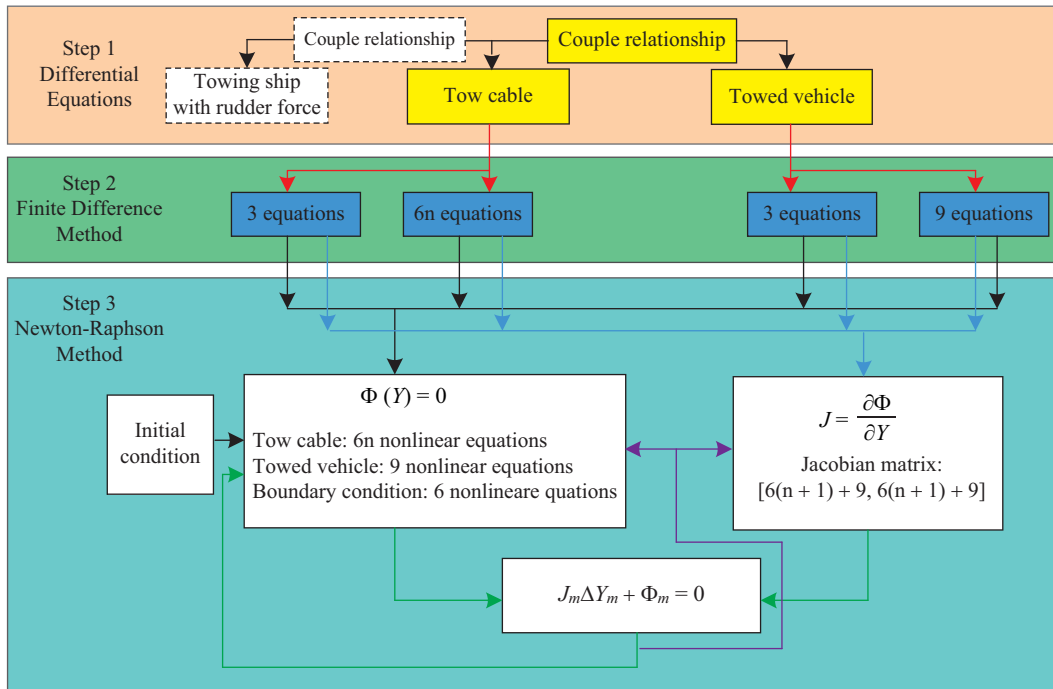
Fig. 2. The flow chart for calculating the nonlinear equations.

and towed vehicle Eqs. (7)-(12) and Eqs. (29)-(31). The second step is discretizing the dynamic model in time and in space using the finite difference method. The third step is the Newton-Raphson iteration scheme to solve the equations.

Denote Y_m an approximate value in the mth iteration for the solution of unknown variables Y, and

$$Y_{m+1} = Y_m + \Delta Y_m \qquad (34)$$

where ΔY_m is found by solving the linear algebraic equations

$$J \Delta Y_m + \Phi_m = 0 \qquad (35)$$

$J = \dfrac{\partial \Phi}{\partial Y}$ is the Jacobian matrix of equation $\Phi(Y) = 0$, and the bracketed subscript m denotes the iteration index.

As shown in the Fig. 2, the towing ship equation with rudder force can be considered in the whole system and the couple relationship between the towing ship with tow cable established using the velocity boundary condition.

II. SIMULATION AND DISCUSSIONS

The above mathematical model has been solved numerically. The results can give the three dimensional shape of the towed system, as well as the kinematic and dynamic properties of cables and the towed vehicle. The direction of a towing ship path, towing speed and attitude of towed vehicle may be changed at any time. Thus the model can be used to predict the dynamic re-
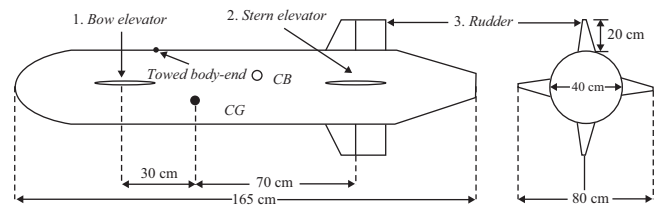
Fig. 3. Physical dimensions of the towed vehicle.

sponse of the system during different maneuvers. In this section numerical simulation are given about the towed system behavior during ship turning maneuvers. The towed vehicle being investigated is assumed to be a circular cylinder with symmetry about its center of uniform mass and it is equipped with a main horizontal control wing, a horizontal and a vertical tail wings (See Fig. 3).

As we known, the 180° and 360° turning maneuvers are two typical representatives in many kind of maneuvers. For demonstration of the validity of the model on describing 3-D hydrodynamic behaviors of towed system during the ship turning maneuvers, examples of towing ship making 180° and 360° turning maneuvers are presented in this section. In the researches (Chapman, 1984; Grosenbaugh, 2007), the authors validated that for the ratio R/L below 1, the depth of towed system varied nonlinearly. In order to check the model systematically, according to the length of tow cable and the capability of towing ship, we defined four turning radiuses. The tow cable and towed vehicle parameters used in the investigation were given in Table 1 and Table 2.

Table 1. Parameters of tow cable.

Water density (kg/m³)	Velocity (kn)	Length (m)	Mass per unit Length (kg/m)	Tangential drag coefficient	Normal drag coefficient	Diameter (m)	Elasticity EA (kN)
1025	3	1000	0.75	0.02	2.00	0.0175	2.625×10^4

Table 2. Parameters of towed vehicle.

Dry mass	Length	Volume	Centre of mass		Centre of buoyancy		Towed vehicle-end	
416 kg	1.65 m	0.28 m³	Fore/aft (X)	0.00 m	Fore/aft (X)	-0.30 m	Fore/aft (X)	0.15 m
			Athwartship (Y)	0.00 m	Athwartship (Y)	0.00 m	Athwartship (Y)	0.00 m
			Vertical (Z)	0.00 m	Vertical (Z)	-0.10 m	Vertical (Z)	-0.20 m
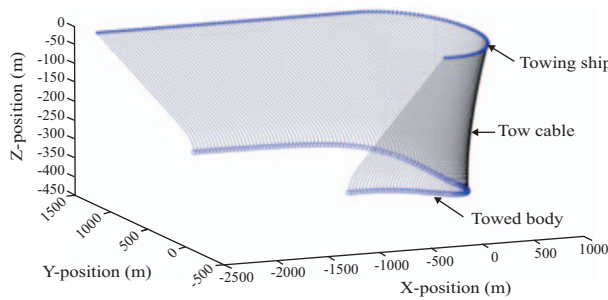
Fig. 4. Time history of cable towed vehicle system configuration during 180° turning maneuvers with ship-turning radius R = 650 m.
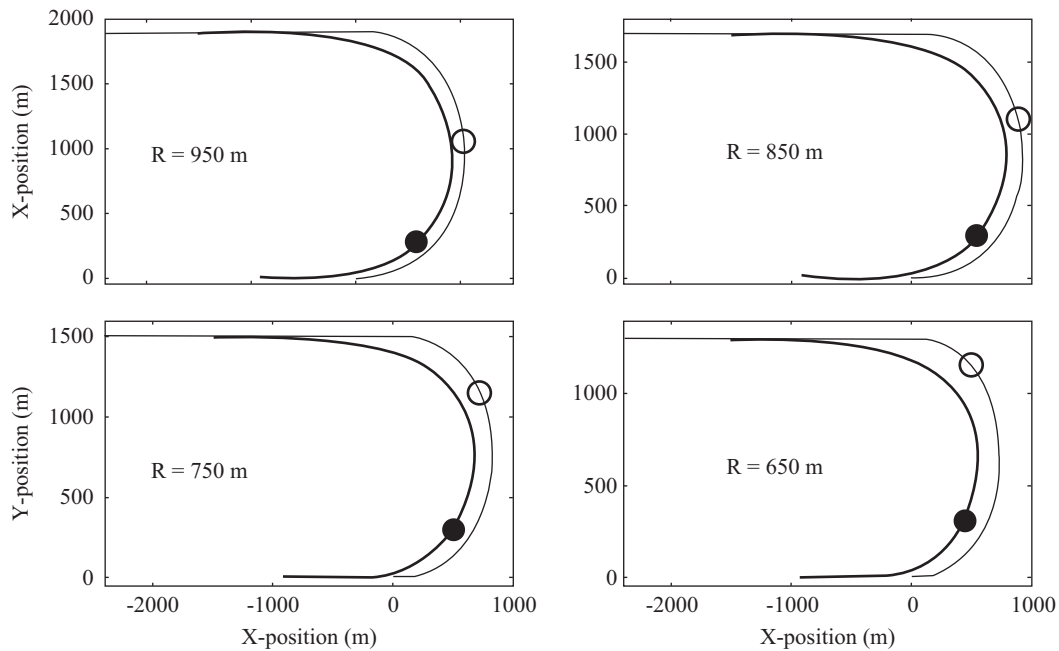
Fig. 5. Horizontal trajectories of towing ship (thin line) and towed vehicle (thick line) during 180° turning maneuvers.

1. 180° Turn Turning Maneuver

In this maneuver, the towing ship starts from a straight tow course and then performs an 180° turn with a radius R = 650 m. After the 180° turn, the ship returns to a straight tow course but in the reverse direction (See Fig. 4). Similarly, we run simulations for three different turning radiuses, i.e., R = 750 m, 850 m, 950 m.

1) Horizontal Trajectory

In the Fig. 5, the horizontal trajectories of the towed vehicle follow the horizontal trajectories of the towing ship in the internal side of the half circles. Fig. 5 shows that the towed vehicle horizontal trajectories are different for different ship turning radiuses. In order to illustrate the differences between the two horizontal trajectories for different turning radiuses, we define dD as
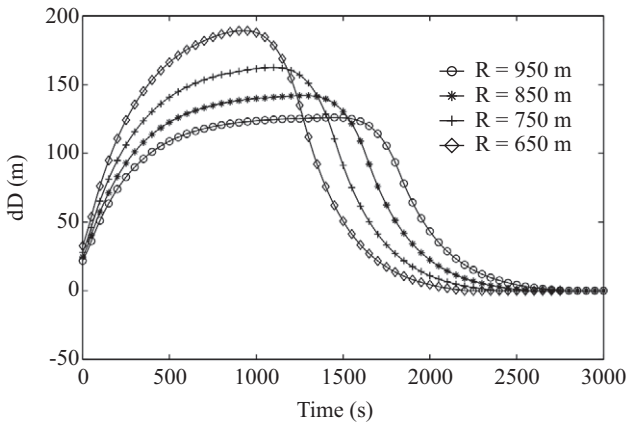
Fig. 6. Least distance between the horizontal trajectories of towing ship (thin line) and towed vehicle (thick line) during 180° turning maneuvers.
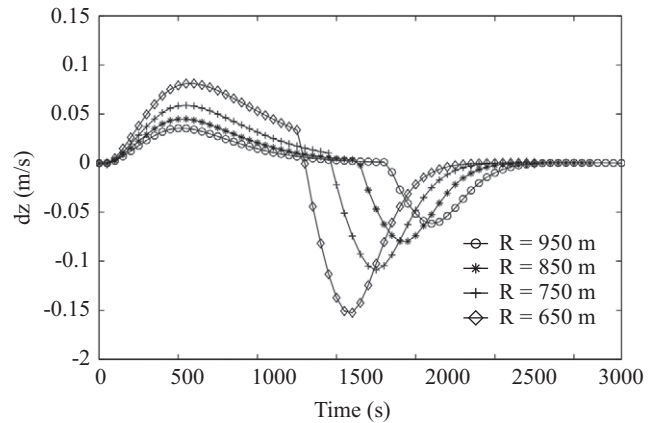

Fig. 8. Time history of towed vehicle depth variation rate during 180° turning maneuvers for different towing ship turning radius.
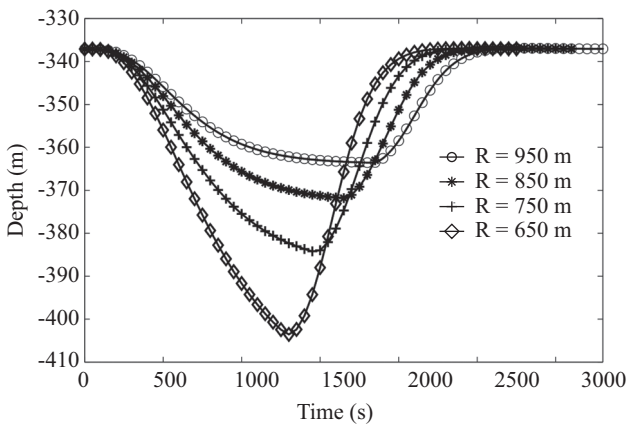

Fig. 7. Time history of towed vehicle depth during 180° turning maneuvers for different towing ship turning radius.
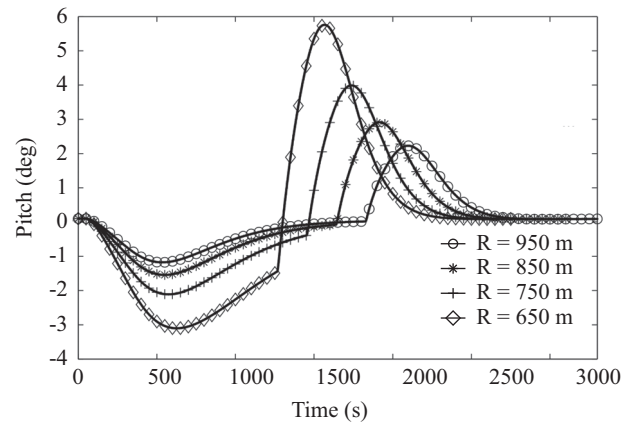

Fig. 9. Time history of towed vehicle pitch angle during 180° turning maneuvers for different towing ship turning radius.

the least distance between the two horizontal trajectories. Fig. 6 shows that the dD increases to maximum and decreases to zero during the turning maneuvers. It means that the two horizontal trajectories will coincide at last. Moreover, for larger turning radius, the variation of dD is smaller and dD is hard to reach a steady-state for this four turning radiuses, when the ship makes 180° turning maneuver. As the turning radius larger enough, the steady-state can be reached.

2) Depth

When the towing ship enters into the 180° turn, the forward towing speed reduces due to radial speed component. As a result, the drag force on the tow cable reduces, and the towed vehicle dives deeper. After the ship exits the turn and moves straight again, the towed vehicle's depth decreases due to the increase of towing speed in its forward axis and returns to the previous depth before the 180° turn (See Fig. 7). It can be seen that for smaller radius of ship 180° turn, the depth variations of the towed vehicle is larger. The depth of towed vehicle never reaches a steady-state during the ship 180° turning maneuver.

We define the dz as the variation rate of towed vehicle depth. The dz increases to positive maximum and then decreases during the towing ship turning maneuver (See Fig. 8). When the towing ship returns to a straight tow course, the dz decreases to negative maximum, which means the depth of towed vehicle become lower. For smaller turning radius, the variation is lager and dz never keeps at zero. This also illustrates that the depth of towed vehicle not reaches a steady-state.

3) Attitude

Accordingly, as the towed vehicle depth changing, the pitch and roll angles of the towed vehicle will vary at the same time. Fig. 9 shows the time history of towed vehicle pitch angle during the towing ship making 180° turning maneuvers. It can be seen that the pitch angle becomes negative at the beginning of the turn, which means that the towed vehicle noses down. Then, the pitch angle increases and is close to a new steady state. As the towing ship returning to the straight tow course, the value of pitch angle increases to a maximum sharply and decreases to the pitch angle of straight tow. Moreover, for larger turning radius, the variation of the pitch angle is smaller.
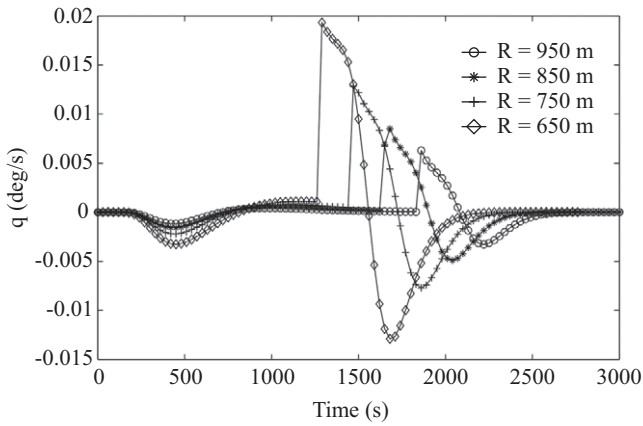
Fig. 10. Time history of towed vehicle pitch angle variation rate during 180° turning for different towing ship turning radius.
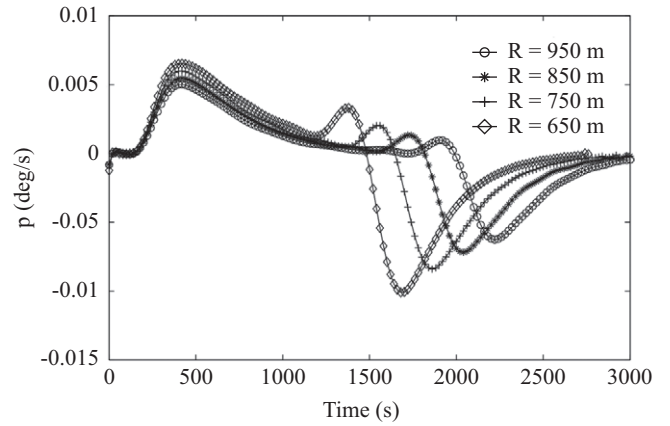

Fig. 12. Time history of roll angle variation rate during 180° turning maneuvers for different towing ship turning radius.
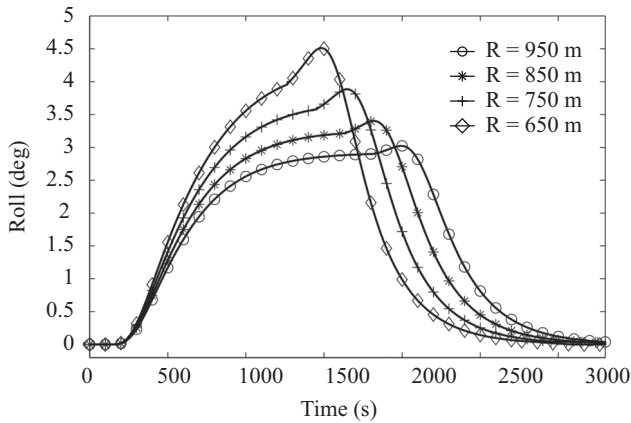

Fig. 11. Time history of roll angle during 180° turning maneuvers for different towing ship turning radius.
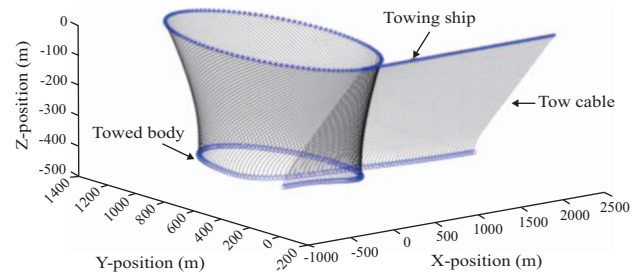

Fig. 13. Time history of cable towed vehicle system configuration during 360° turning maneuvers for different towing ship turning radius.

In order to illustrate the variation rate of pitch angle with different turning radius, we define q as the variation rate of the pitch angle. Fig. 10 shows that the value q varies during the towing ship turning maneuvers. It can be found that the variation of pitch angle is nonlinear also and it is a function of turning radius. For larger turning radius, the variation of q is smaller. The value of q is hard to keep at zero, which means that the pitch angle changes all the time during the 180° turning maneuver.

In addition, with the variation of towed vehicle pitch angle, the roll angle increases to a maximum value during the ship turning (See Fig. 11), but never reach a steady-state. As the ship returns to straight tow, the value of roll angle decreases to zero. Fig. 12 shows the variation of roll angle p. For larger turning radius, the value of p is smaller and never reach to zero during the 180° turning maneuvers.

2. 360° Turning Maneuver

In this maneuver, the ship starts from a straight tow, completes a 360° turn of radius R = 650 m, and then returns to a straight tow again, see Fig. 13. Similarly, we simulated three different turning radiuses R = 750 m, 850 m, 950 m.

1) Horizontal Trajectory

Depending on the towing ship, the towed vehicle will complete a full circular turn. The horizontal trajectories of towed vehicle are inside of the towing ship horizontal trajectories. Fig. 14 shows that the radius of towed vehicle is smaller than the ship turning radius. It can be found that the least distance between two horizontal trajectories in the Fig. 15. The value of dD can reach a steady-state, during the towing ship turning maneuvers (R = 950, 850, 750 m). Moreover, the value of dD is larger with a smaller turning radius. For larger of the ship turning radius, the towed vehicle turning radius is close to the ship turning radius.

2) Depth

As the ship beginning to turn, the towed vehicle increases to a maximum and then rises back to the original straight-tow equilibrium depth (refer to Fig. 16). For larger ship turning radius (R = 950, 850, 750 m), the towed vehicle sinks to its steady-state turning depth before rising back to the former steady-state, straight-
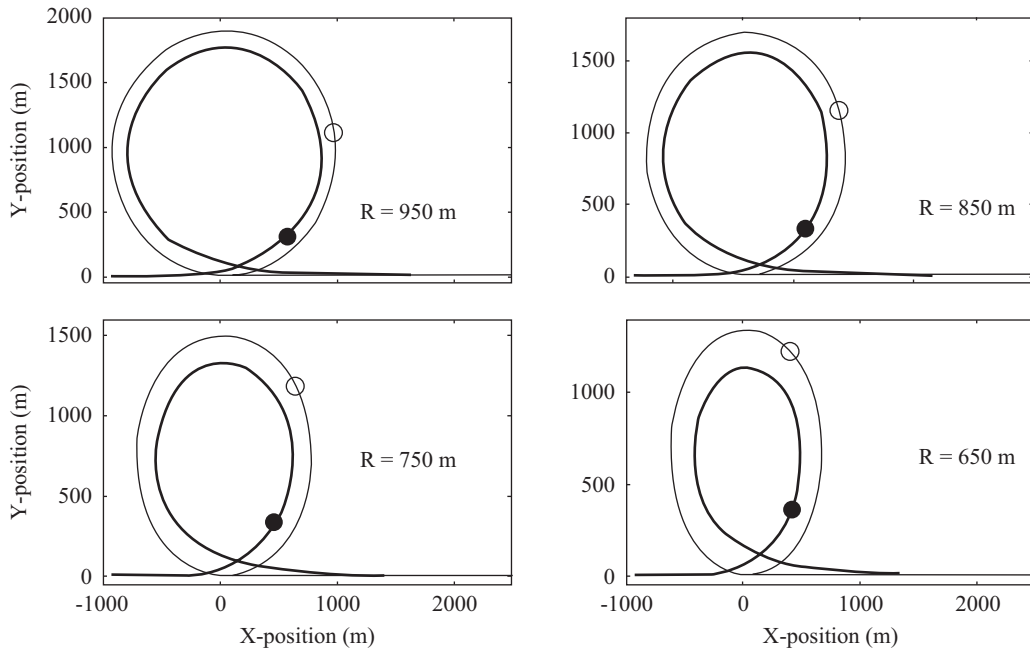
Fig. 14. Horizontal trajectories of towing ship (thin line) and towed vehicle (thick line) during 360° turning maneuvers.
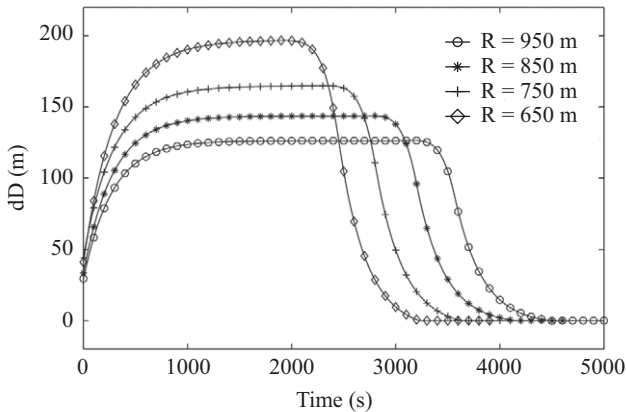

Fig. 15. Least distance between the trajectories of towing ship (thin line) and towed vehicle (thick line) during 360° turning maneuvers.
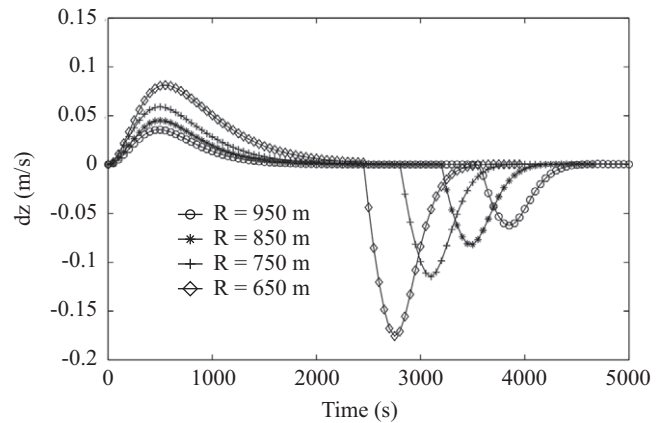

Fig. 17. Time history of variation rate of towed vehicle depth during 360° turning maneuvers for different towing ship turning radius.
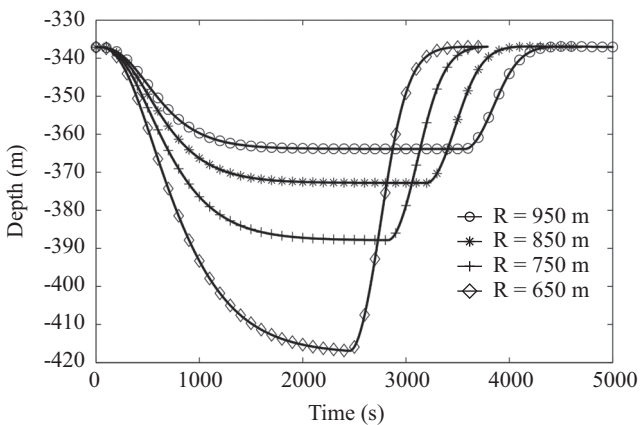

Fig. 16. Time history of towed vehicle depth during 360° turning maneuvers for different towing ship turning radius.
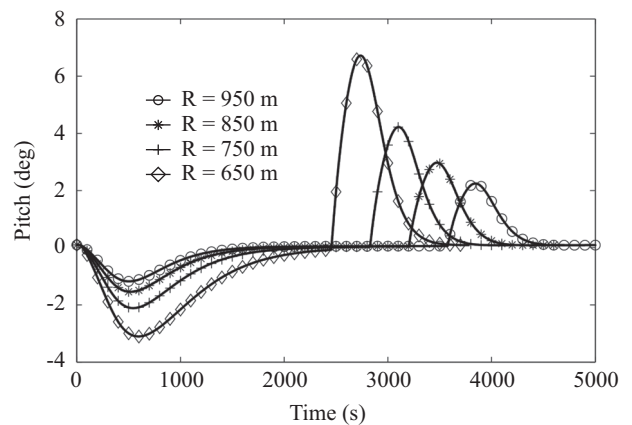

Fig. 18. Time history of towed vehicle pitch angle during 360° turning maneuvers for different towing ship turning radius.
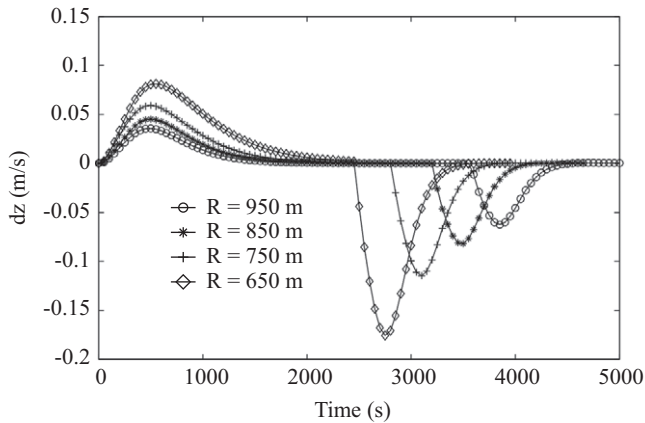
Fig. 19. Time history of variation rate of towed vehicle depth during 360° turning maneuvers for different towing ship turning radius.
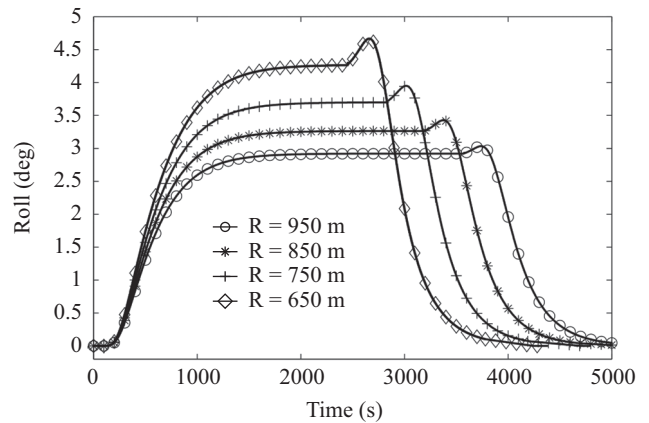

Fig. 20. Time history of towed vehicle roll angle during 360° turning maneuvers for different towing ship turning radius.

line depth. Moreover, for larger ship turning radius, the decrease in the towed vehicle depth is a small fraction of the original of the straight-tow equilibrium depth and it reaches to the steady state more quickly. For small turning radius (R = 650 m), the depth of towed vehicle never reach to a new steady-state.

Fig. 17 shows the variation rate of towed vehicle depth is given out. It can be seen that for larger turning radius (R = 950, 850, 750 m), the variation of dz is smaller and it can reach to zero more quickly. For smaller turning radius (R = 650 m), the variation of dz is larger and is hardly reach to zero, which means that the depth of towed vehicle changes during the whole turning maneuvers. It shows that the variation of towed vehicle depth depends on the ship turning radius.

3) Attitude

Fig. 18 shows that at beginning of the 360° turning maneuver, the towed vehicle noses down to a maximum and then rises to new state. After the towing ship complete the full circular turn, the towed vehicle noses up and returns to the original straight-tow equilibrium pitch angle. Moreover, it can be found that for larger ship turning radius, the variation of towed vehicle pitch angle is smaller and it can reach a new steady of pitch angle more easily. In the Fig. 19, it can be seen that the value of q is a function of ship turning radius. For lager ship turning radius, the variation of q is smaller. For larger turning radius (R = 950, 850, 750 m), the value of q can reach to zero, which means that the pitch angle can reach a new steady-state during the 360° turning maneuver.

Fig. 20 shows the roll angle of towed vehicle varies during the ship 360° turning maneuvers. During the ship turn, the state of towed vehicle is starboard and after the towing ship makes a full circular turn, the roll angle of the towed vehicle decreases to zero. It can be found that for smaller of the ship turning radius, the variation of the roll angle is lager. This variation rate of roll angle p can be seen from the Fig. 21. In the Fig. 21, we can see that the variation rate of roll angle is lager for smaller radius and the value of p can reach to zero for the larger turning radius (R = 950, 850, 750 m).
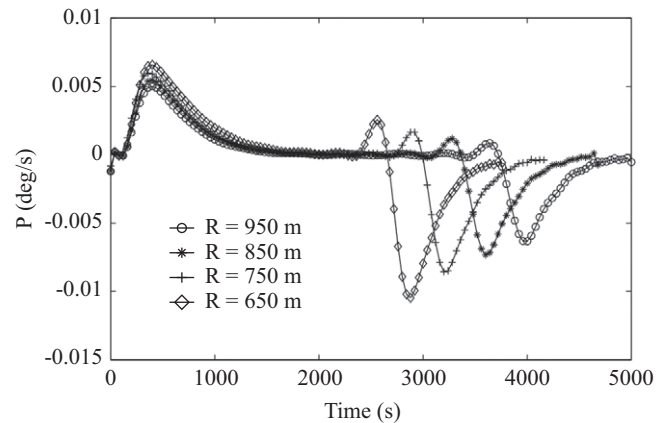

Fig. 21. Time history of roll angle variation rate during 360° turning maneuvers for different towing ship turning radius.

III. CONCLUSIONS

A numerical scheme has been proposed to predict the behavior of towed system which results from the towing ship changing course from a straight-tow trajectory to a turning maneuver at a constant radius. We use the computer program based on the model to simulate the depth and attitude of towed system during the ship 180° and 360° turning maneuvers. From the present overall results, we can draw the following conclusions:

(1) For lager of ship turning radius, the horizontal trajectory of towed vehicle is closer to the horizontal trajectory of the towing ship. During the 180° turning maneuvers for the four turning radiuses, the least distance between the two horizontal trajectories can't reach steady-state, but the values can reach steady-states during the 360° turning maneuvers for larger radius (R = 950, 850, 750 m).

(2) For larger ship turning radius, the decrease in the towed vehicle depth is a small fraction of the original of the straight-tow equilibrium depth. In fact, the towed vehicle never reached the steady-state depth during the 180° maneuvers

Journal of Marine Science and Technology, Vol. 25, No. 4 (2017)

for the turning radius used in this steady and during the 360° turning maneuvers, the steady-state can be achieved for larger turning radiuses (R = 950, 850, 750 m).

(3) During the 180° and 360° turning maneuvers, the attitude of towed vehicle vary. For the drag tension reduced at the beginning of turning maneuvers, the pitch angle of towed vehicle becomes negative. With the increase of the velocity in its forward axis, the pitch angle increases to a maximum value and returns the original of the straight-tow equilibrium value. The roll angle of towed vehicle varies during the ship turning maneuvers also. The state of towed vehicle increases to maximum and after the towing ship makes a full circular turn, the roll angle of the towed vehicle decreases to zero. The variation of towed vehicle attitude is determined by the characteristics of the turning maneuvers. For larger turning radius, the variation of attitude is larger. The attitude of towed vehicle never reach steady-state during the 180° turning maneuver, but this value can reach a new steady-state during the 360° turning maneuver with lager turning radius (R = 950, 850, 750 m).

The mathematical model provides a good algorithm for predicting the behavior of towed system. A suitable turning radius can be calculated, which can guarantee the depth and attitude variations meeting the requirements of the towed system. Moreover, the model presented in this paper can easily be extended to predicting behavior of towed system during other types of ship maneuvers.

REFERENCES

Ablow, C. M. and S. Schechter (1983). Numerical simulation of undersea cable dynamics. Ocean Engineering 10, 443-457.

Chapman, D. A. (1984). The towed cable behavior during ship turning manoeuvers. Ocean Engineering 11, 327-361.

Choo, Y. and M. J. Casarella (1972). Configuration of a towline attacthed to a vehicle moving in a circular path. Journal of Hydronautics 6, 51-57.

Feng, Z. and R. Allen (2004). Evalauation of the effects of the communication cable on the dynamics of an underwater flight vehicle. Ocean Engineering 31, 1019-1035.

Fernandez, J., D. Cook and J. Christoff (2002). Motion compensation technique for wide beam synthrtic aperture sonar[J]. The Journal of the Acoustical Society of America 111(5), 2450-2457.

Fossen, T. I. (1994). Guidance and Control of OceanVehicles. 1994, Wiley, England.

Fossen, T. I. (2002). Marine Control Systems Guidance, Navigation, and Control of Ships, Rigs and Underwater Vehicles. Marine Cybernetics.

Georgiades, C., M. Nahon and M. Buehler (2009). Simulation of an underwater hexapod robot. Ocean Engineering 36, 39-47.

Grosenbaugh, M. A. (2007). Tansient behavior of towed cable systems during ship turning maneuvers. Ocean Engineering 34, 1532-1542.

Han, X. V., J. D. Samuel and F. K. Fletcher (2013). Track-before-detect for an active towed array sonar. Proceeding of Acoustics 2013, Victor Harbor, Australia: 1-7.

Montefalcone, M., A. Rovere, V. Parravicini, G. Albertelli, C. Morri and C. N. Bianchi (2013). Evaluating change in seagrass meadows: A time-framed comparison of Side Scan Sonar maps. Aquatic Botany 104, 204-212.

Narasimhan, M., S. N. Singh (2006). Adaptive optimal control of an autonomous underwater vehicle in the dive plane using dorsal fins. Ocean Engineering 33, 404-416.

VanZwieten, J., F. R. Driscoll, A. Leonessa and G. Deane (2006). Design of a prototype ocean current turbine-Part I: mathematical modeling and dynamics simulation. Ocean Engineering 3, 1485-1521.

Wang, Z. and S. Gang (2015). Parameters influence on maneuvered towed cable system dynamics. Applied Ocean Research 49, 27-41.

Yuan, Z., L. Jin and W. Chi (2014). Finite difference method for solving the nonlinear dynamic equation of underwater towed system. International Journal of Computational Methods 11(4), 85-89.

Yuan, Z., L. Jin and W. Chi (2016). Research on the coupling model of underwater towed system. Journal of Ship Mechanics 26(10), 1252-1261.